

Flavor quarks in AdS₄ and gauge/gravity correspondenceKazuo Ghoroku,^{1,*} Masafumi Ishihara,^{2,†} and Akihiro Nakamura^{3,‡}¹*Fukuoka Institute of Technology, Wajiro, Higashi-ku, Fukuoka 811-0295, Japan*²*Department of Physics, Kyushu University, Hakozaki, Higashi-ku, Fukuoka 812-8581, Japan*³*Department of Physics, Kagoshima University, Korimoto, 1-21-35, Kagoshima 890-0065, Japan*

(Received 21 December 2006; published 14 February 2007)

The nonperturbative properties of gauge theories in AdS₄ are studied in dual supergravity by including light flavor quarks, which are introduced by a D7-brane embedding. Contrary to the Minkowski and dS₄, the dilaton does not play any important dynamical role in the AdS₄ case, and the characteristic properties like quark confinement and chiral symmetry breaking are realized mainly due to the geometry AdS₄. The possible hadron spectra are also examined, and we find that the meson spectra are well described by the formula given by the field theory in AdS₄, but the characteristic mass scale is modified by the gauge interactions for excited states.

DOI: [10.1103/PhysRevD.75.046005](https://doi.org/10.1103/PhysRevD.75.046005)

PACS numbers: 11.25.Mj, 04.50.+h, 11.25.Hf, 11.30.Rd

I. INTRODUCTION

Recently, based on gauge/gravity correspondence [1], many nonperturbative properties of Yang-Mills (YM) theories with quarks have been uncovered in terms of superstring theory [2–11]. In these approaches, flavor quarks are introduced by embedding probe D7-brane(s) in an appropriate bulk 10d background, which could describe the QCD type of Yang-Mills theory, and many successful results have been obtained for the properties of quarks and their bound states.

Up to now, almost all efforts have been devoted to the study of gauge theory in 4d Minkowski space-time. Previously, we extended our analysis to gauge theory in 4d de Sitter space, dS₄, and many interesting properties were found [12,13]. Here we, furthermore, extend the analysis into the case of 4d anti-de Sitter space-time, AdS₄, which is embedded in the 10d bulk. The quantum field theory in the AdS₄ has been studied in [14], and the discrete mass spectra of the scalar field have been found under the reflective boundary conditions for the universal covering space CAdS. The same mass formula for the massive spin two states, which corresponds to the glueball states in gauge theory, is found from 5d AdS analysis by demanding the normalizability of the wave function in the fifth direction [15]. This implies the usefulness of the holographic approach to gauge theory in AdS₄. In [15], the existence of the massive graviton in AdS₄ has been pointed out in a three-brane where gravity couples with conformal field theories (CFT). And this observation has been further studied by Porrati as a ‘‘Higgs phenomena’’ driven by dynamics in geometry AdS₄ [16,17].

Here we concentrate our attention on the properties of flavor quarks which couple to the CFT embedded in AdS₄, which would give a strong constraint on the dynamics of

quarks interacting with deformed CFT as seen in the case of gravity. The analysis is performed according to the formulation given before for the case of dS₄ [12].

In Sec. II, we give the setting of our model for the present study. In Sec. III, the potential between the quark and antiquark and the effective quark mass are studied through the Wilson-Polyakov loop estimate. In Sec. IV, the embedding of the D7-brane and the chiral symmetry breaking are discussed. In Sec. V, the possible bound states for the meson and baryon are discussed. The meson spectra are compared with the formula given by the field theory in AdS₄. The summary is given in the final section.

II. BACKGROUND GEOMETRY

We start from the type IIB supergravity with the following bosonic action,

$$S = \frac{1}{2\kappa^2} \int d^{10}x \sqrt{-g} \left(R - \frac{1}{2} (\partial\Phi)^2 + \frac{1}{2} e^{2\Phi} (\partial\chi)^2 - \frac{1}{4 \cdot 5!} F_{(5)}^2 \right), \quad (1)$$

where other fields are neglected since we do not need them, and χ is Wick rotated. By taking the ansatz for $F_{(5)}$, $F_{m_1 \dots m_5} = -\sqrt{\Lambda}/2 \epsilon_{m_1 \dots m_5}$ and $F_{\alpha_1 \dots \alpha_5} = \sqrt{\Lambda}/2 \epsilon_{\alpha_1 \dots \alpha_5}$ [18–20], and for the 10d metric as $M_5 \times S^5$ or $ds^2 = g_{mn} dx^m dx^n + g_{\alpha\beta} dx^\alpha dx^\beta$,¹ the equations of motion are given as

$$R_{mn} = -\Lambda g_{mn} + \frac{1}{2} \partial_m \Phi \partial_n \Phi - \frac{1}{2} e^{2\Phi} \partial_m \chi \partial_n \chi, \quad (2)$$

$$\frac{1}{\sqrt{-g}} \partial_m (\sqrt{-g} g^{mn} \partial_n \Phi) = -e^{2\Phi} \partial_m \chi \partial_n \chi g^{mn}, \quad (3)$$

*Email address: gouroku@dontaku.fit.ac.jp†Email address: masafumi@higgs.phys.kyushu-u.ac.jp‡Email address: nakamura@sci.kagoshima-u.ac.jp¹Here m, n denote $\mu, \nu = 0-3$ and the direction of r , the fifth coordinate. And $\alpha, \beta = 5-9$.

$$\frac{1}{\sqrt{-g}} \partial_m (\sqrt{-g} g^{mn} e^{2\Phi} \partial_n \chi) = 0, \quad (4)$$

$$R_{\alpha\beta} = \Lambda g_{\alpha\beta}. \quad (5)$$

Using the ansatz

$$\chi = -e^{-\Phi} + \chi_0, \quad (6)$$

where χ_0 is a constant, Eq. (2) is written as

$$R_{mn} = -\Lambda g_{mn}. \quad (7)$$

We notice that this equation (7) is independent of the fields Φ and χ . This implies the usual 5d AdS solution, and we know that the four dimensional slice perpendicular to the fifth coordinate r is taken as AdS₄ as well as Minkowski or dS₄. Here we consider the case of AdS₄ embedded in AdS₅.

After adopting the solution AdS₄ embedded in AdS₅ for the metric, Φ and χ are obtained from (3) and (6). Thus we obtain the following solution,

$$\begin{aligned} ds_{10}^2 &= G_{MN} dX^M dX^N \\ &= e^{\Phi/2} \left\{ \frac{r^2}{R^2} A^2 (-dt^2 + a(t)^2 \gamma(x)^2 (dx^i)^2) \right. \\ &\quad \left. + \frac{R^2}{r^2} dr^2 + R^2 d\Omega_3^2 \right\}, \end{aligned} \quad (8)$$

$$\begin{aligned} e^\Phi &= 1 + \frac{q}{6} \left(1 - \frac{1 - (r_0/r)^2}{(1 + (r_0/r)^2)} \left[1 + \frac{2(r_0/r)^2}{(1 + (r_0/r)^2)^2} \right] \right), \\ \chi &= -e^{-\Phi} + \chi_0, \end{aligned} \quad (9)$$

$$\begin{aligned} A &= 1 + \left(\frac{r_0}{r} \right)^2, \quad a(t) = \frac{R^2}{2r_0} \sin \left(2 \frac{r_0}{R^2} t \right), \\ \gamma(x) &= \frac{1}{1 - x_i x^i / (4\tilde{r}_0^2)}, \end{aligned} \quad (10)$$

where $M, N = 0 \sim 9$, $R = \sqrt{\Lambda}/2 = (4\pi N_c)^{1/4}$ and \tilde{r}_0 is an arbitrary scale factor. We comment on two other integration constants, r_0 and q . First, r_0 has nothing to do with the horizon since there is no horizon in the present solution and r is considered in all the region of $0 < r < \infty$ contrary to the dS₄ case. This parameter r_0 is, however, important since it is related to the 4d cosmological constant λ , which is negative, as follows

$$-\lambda = 4 \frac{r_0^2}{R^4}. \quad (11)$$

And q is a constant which corresponds to the gauge field condensate [10] defined as the vacuum expectation value of the gauge-field squared as

$$q \equiv \tilde{q}/r_0^4 = \langle F_{\mu\nu}^2 \rangle / r_0^4. \quad (12)$$

We assume that $\langle F_{\mu\nu}^2 \rangle = \tilde{q}$ is finite, and other field configurations are set to be zero.

Our model is based on type IIB supergravity, and we solved the equations of motion for the dilaton and axion with the ansatz (6). In this case, the condition for the supersymmetry of the solution is reduced to the presence of the Killing spinor u [18,20] which satisfies the following equation in terms of the 10d gamma matrices Γ_M ,

$$\delta \Psi_M = \left(D_M - \frac{\sqrt{\Lambda}}{4} \Gamma_M \right) u = 0, \quad (13)$$

where Ψ_M denotes the gravitino and $D_M = \partial_M + \frac{1}{4} \omega_M^{AB} \Gamma_A \Gamma_B$. The equation for the dilatino, $\delta \lambda = 0$, is satisfied due to the ansatz (6). The S^5 part of (13) is obtained as in the case of AdS₅ \times S^5 [21]. For the AdS₅ part, the condition is modified due to the metric of AdS₄. In this case, the covariant derivatives are written as

$$D_r u = \partial_r u, \quad (14)$$

$$D_0 u = \left(\partial_0 - \frac{\mu}{2} \left(\frac{1 - (r_0/r)^2}{1 + (r_0/r)^2} \right) \Gamma_0 \Gamma_r \right) u, \quad (15)$$

$$\begin{aligned} D_i u &= \left(\partial_i - \frac{\gamma(x)}{2} \partial_0 a(t) \hat{\Gamma}_i \hat{\Gamma}_0 + \frac{1}{2\gamma(x)} \partial_j \gamma(x) \hat{\Gamma}_i \hat{\Gamma}_j \right. \\ &\quad \left. - \frac{\mu}{2a(t)\gamma(x)} \left(\frac{1 - (r_0/r)^2}{1 + (r_0/r)^2} \right) \Gamma_i \Gamma_r \right) u, \end{aligned} \quad (16)$$

where $\hat{\Gamma}_M$ denotes the local Lorentz constant gamma matrix. From these results for finite r_0 , we easily find that there is no Killing spinor, the solution of (13), of the form $u = f(y, x^\mu) u_0$, where u_0 is some constant spinor. In other words, there is no supersymmetry in the present case. We notice that the supersymmetry is also broken by our D7-brane embedding since the κ symmetry of the D7-brane action is lost [10] when the chiral symmetry is broken.

In this model, the four dimensional slice represents the AdS₄ universe characterized by the 4d cosmological constant λ . Then the bulk gravity describes the gauge theory in AdS₄. The gauge coupling constant in the present model is finite in the limits of both ultraviolet and infrared,

$$g_{\text{YM}}^2 = e^\Phi = \begin{cases} 1 + \frac{q}{3} - q \left(\frac{r}{r_0} \right)^4 & \text{for } r \rightarrow 0 \text{ (IR limit),} \\ 1 + q \left(\frac{r_0}{r} \right)^4 & \text{for } r \rightarrow \infty \text{ (UV limit).} \end{cases} \quad (17)$$

Meanwhile, in the limit of Minkowski space or the limit of $r_0 \rightarrow 0$, we have $g_{\text{YM}}^2 = 1 + \frac{\tilde{q}}{r^4}$, which is equivalent to the supersymmetric solution given previously [10]. In this case, the quark is confined since the YM coupling constant becomes very strong in the infrared limit, $r \rightarrow 0$ for $\tilde{q} > 0$. But, for finite r_0 or in the AdS₄ space-time, in the limit $r \rightarrow 0$, we find $g_{\text{YM}}^2 \rightarrow 1 + \frac{q}{3}$, and it is not large enough for the quark confinement. However, the confinement is seen in this case due to the behavior of the warp factor $A(r)$ since it diverges at $r = 0$ for finite r_0 . This is assured by the calculation of the Wilson loop. Then the result for the

quark confinement is independent of the value of q , which is needed in the Minkowski space-time for the quark confinement, in AdS₄.

III. WILSON LOOP AND QUARK CONFINEMENT

We study here the quark confinement through the Wilson-Polyakov loop in $SU(N)$ gauge theory, defined as $W = \frac{1}{N} \text{Tr} P e^{i \int A_0 dt}$. Then the quark-antiquark potential $V_{q\bar{q}}$ is derived from the expectation value of a parallel Wilson-Polyakov loop. From the dual gravity side, it is represented as

$$\langle W \rangle \sim e^{-S}, \quad (18)$$

in terms of the Nambu-Goto action

$$S = -\frac{1}{2\pi\alpha'} \int d\tau d\sigma \sqrt{-\text{deth}_{ab}}, \quad (19)$$

with the induced metric $h_{ab} = G_{\mu\nu} \partial_a X^\mu \partial_b X^\nu$. The string world sheet is parametrized by σ, τ .

We examine quark-antiquark potentials in the background given above. To study possible static string configurations of a quark-antiquark pair, we choose $X^0 = t = \tau$ and $X^1 = x^1 = \sigma$; then the Nambu-Goto Lagrangian in the background (8) becomes

$$L_{\text{NG}} = -\frac{1}{2\pi\alpha'} \int d\sigma e^{\Phi/2} A(r) \times \sqrt{r'^2 + \left(\frac{r}{R}\right)^4 (A(r)a(t)\gamma(x))^2}, \quad (20)$$

where the prime denotes the derivative with respect to σ . The test string has two possible configurations: (i) a pair of parallel strings, which connect the D7- and D3-branes, and (ii) a U-shaped string whose two end points are on the D7-brane.

First, we study configuration (i). In this case, the parallel strings have no correlation with each other; then the total energy of this configuration is 2 times that of one effective quark mass, \tilde{m}_q . It is given by a string configuration which stretches between $r = 0$ and r_{max} , which denote the position of D3- and D7-branes, respectively. So we can take $r = \sigma$, and then we obtain

$$\tilde{m}_q = \frac{1}{2\pi\alpha'} \int_0^{r_{\text{max}}} dr e^{\Phi/2} A(r). \quad (21)$$

Near $r = 0$, the integrand is approximated as $e^{\Phi/2} A(r) \sim \sqrt{1 + \frac{q}{3} \left(\frac{r_0}{r}\right)^2}$; then we find that \tilde{m}_q diverges as

$$\tilde{m}_q \sim \sqrt{1 + \frac{q}{3} \frac{r_0^2}{r}} \Big|_{r \rightarrow 0} \rightarrow \infty. \quad (22)$$

Thus configuration (i) cannot be realized. In other words, the quark should be confined. And this result is satisfied

even if $q = 0$; then the confinement is caused only by the gravitational effect.

The next check of the quark confinement is to see the area law through the U-shaped configuration. The energy of this configuration is obtained from (20) as

$$E = -L_{\text{NG}} = \frac{1}{2\pi\alpha'} \int d\tilde{\sigma} e^{\Phi/2} A(r) \sqrt{(\partial_{\tilde{\sigma}} r)^2 + \left(\frac{r}{R}\right)^4 (A(r))^2} \quad (23)$$

$$= \frac{1}{2\pi\alpha'} \int d\tilde{\sigma} n \sqrt{1 + \left(\frac{R^2}{r^2 A} \partial_{\tilde{\sigma}} r\right)^2}, \quad (24)$$

where

$$n = e^{\Phi/2} \left(\frac{rA}{R}\right)^2 \quad (25)$$

and

$$\tilde{\sigma} = a(t) \int d\sigma \gamma(\sigma) = a(t) \int d\sigma \frac{1}{1 - \sigma^2/4}. \quad (26)$$

Here the coordinates of the string action are set as $x^1 = \sigma$, $x^2 = x^3 = 0$. In this case, we obtain

$$\tilde{\sigma} = 4a(t) \tanh^{-1} \left(\tan \left(\frac{\theta}{2} \right) \right), \quad \sigma = 2 \cos(\theta), \quad (27)$$

where $0 \leq \theta < \pi/2$, and we find $0 \leq \tilde{\sigma} < \infty$. The physical distance between the quark and antiquark is measured by $\tilde{\sigma}$ rather than σ which is restricted as $-2 < \sigma < 2$ in our definition of the metric given by (8).

Then the distance between the quark and the antiquark at $t = 0$ is given as

$$\tilde{L} = 2 \int_{\tilde{\sigma}_{\text{min}}}^{\tilde{\sigma}_{\text{max}}} d\tilde{\sigma} = 2(\tilde{\sigma}_{\text{min}} - \tilde{\sigma}_{\text{max}}), \quad (28)$$

where $\tilde{\sigma}_{\text{min}} = \tilde{\sigma}(r_{\text{min}})$, $\tilde{\sigma}_{\text{max}} = \tilde{\sigma}(r_{\text{max}})$, and r_{min} is determined as $\partial_{\tilde{\sigma}} r|_{r_{\text{min}}} = 0$. So r_{min} gives a midpoint of the U-shaped string. On the other hand, r_{max} is given by the position of the D7-brane, the end points of the U-shaped string.

Before giving the numerical estimation of the Wilson loop, we give an analytic approximate estimation according to the method given by Gubser [22]. Equation (24) can be approximately evaluated in terms of the classical solution for r , say $r^*(\tilde{\sigma})$, which minimizes E . And it is approximated by the global minimum of the function n with respect to r . For this solution, we expect $\partial_{\tilde{\sigma}} r^* \sim 0$ for a wide range of σ for large \tilde{L} . Then we obtain

$$E \sim \frac{n(r^*)}{2\pi\alpha'} \tilde{L}, \quad (29)$$

and this implies the linear potential between the quark and antiquark. For the case of small q , we obtain

$$r^* = r_0 \left(1 + \frac{q}{16} + \dots \right), \quad (30)$$

$$n(r^*) = |\lambda| R^2 \left(1 + \frac{q}{12} + \dots \right), \quad (31)$$

where we notice $\lambda = -4r_0^2/R^4$. After all, we find the tension τ_U of the U-shaped string configuration as

$$\tau_U = \frac{|\lambda| R^2}{2\pi\alpha'} \left(1 + \frac{q}{12} + \dots \right). \quad (32)$$

As expected, the tension is finite even if $q = 0$, and λ is the

essential factor to obtain the linear potential or the quark confinement. The relation of (29) is explicitly shown by the numerical calculation.

From the Lagrangian (20), we find the following relation,

$$e^{\Phi/2} \frac{1}{\sqrt{(r/R)^4 A^2(r) + (dr/d\bar{\sigma})^2}} \left(\frac{r}{R} \right)^4 A^3(r) = h, \quad (33)$$

where h denotes a constant of motion. Taking $h = e^{\Phi/2} \left(\frac{r}{R} \right)^2 A^2(r) |_{r_{\min}}$, we get

$$\tilde{L} = 2R^2 \int_{r_{\min}}^{r_{\max}} dr \frac{1}{r^2 A(r) \sqrt{e^{\Phi(r)} r^4 A(r)^4 / (e^{\Phi(r_{\min})} r_{\min}^4 A(r_{\min})^4) - 1}}, \quad (34)$$

$$E = \frac{1}{\pi\alpha'} \int_{r_{\min}}^{r_{\max}} dr \frac{A(r) e^{\Phi(r)/2}}{\sqrt{1 - e^{\Phi(r_{\min})} r_{\min}^4 A(r_{\min})^4 / (e^{\Phi(r)} r^4 A(r)^4)}}. \quad (35)$$

Figure 1 shows the dependence of the energy E on the distance \tilde{L} at the finite cosmological constant $\lambda (= -4)$ for $q = 1$ and $q = 0$. In both cases, we find the linear potential, and the tension given by Eq. (32) is assured. We should notice that this confinement is realized even if $q = 0$, so the gauge interactions are not essential in this case.

Here we notice that the parameter r_{\min} is introduced instead of h , defined in (34), in the above calculation. When r_{\min} approaches r_0 , $f(r_{\min}) \equiv e^{\Phi(r_{\min})} r_{\min}^4 A(r_{\min})^4$ approaches its minimum value. For small q , it is realized at

$$r = r_0 \left(1 + q/16 + \dots \right) \equiv r_M.$$

Then, for $r_{\min} = r_M$, \tilde{L} diverges as

$$\tilde{L} \sim -\frac{2R^2}{r_M^2 A(r_M)} \sqrt{\frac{2f(r_M)}{f''(r_M)}} \log(r - r_M) |_{r \rightarrow r_M}. \quad (36)$$

Therefore, it is enough to consider r_{\min} in the range of

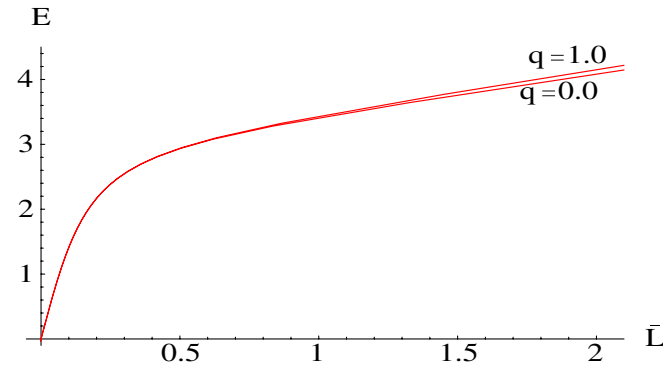


FIG. 1 (color online). Plots of E vs \tilde{L} at $q = 1$ and $q = 0$ for $\lambda = -4$, $R = 1$ (GeV^{-1}), $r_{\max} = 10$ (GeV^{-1}), and $\alpha' = 1$ (GeV^{-2}).

$r_{\min} > r_M$ in order to see the behavior of the U-shaped Wilson loop configuration. On the other hand, we cannot find the U-shaped Wilson loop when we enter into the region of $r_{\min} < r_M$. Instead, we find an upended shaped one in which r_{\min} is the top of the string. So the end points go to $r = 0$ not to r_{\max} . We do not consider this unphysical configuration. Therefore, the natural configuration is obtained when the D7-brane position r_{\max} is taken as $r_{\max} > r_{\min} > r_M$. This point is assured in the next section.

IV. D7-BRANE EMBEDDING AND CHIRAL SYMMETRY

The flavor quarks are introduced by embedding D7-brane(s) in the following rewritten background,

$$ds_{10}^2 = e^{\Phi/2} \left\{ \frac{r^2}{R^2} A^2 (-dt^2 + \gamma(x)^2 a(t)^2 (dx^i)^2) + \frac{R^2}{r^2} (d\rho^2 + \rho^2 d\Omega_3^2 + (dX^8)^2 + (dX^9)^2) \right\}, \quad (37)$$

where $r^2 = \rho^2 + (X^8)^2 + (X^9)^2$. Then the induced metric for the D7-brane is obtained as

$$ds_8^2 = e^{\Phi/2} \left\{ \frac{r^2}{R^2} A^2 (-dt^2 + \gamma(x)^2 a(t)^2 (dx^i)^2) + \frac{R^2}{r^2} ((1 + (\partial_\rho w)^2) d\rho^2 + \rho^2 d\Omega_3^2) \right\}, \quad (38)$$

where we set $X^9 = 0$ and $X^8 = w(\rho)$ without loss of generality due to the rotational invariance in the X^8 - X^9 plane. Then, the effective D7-brane action is given as

$$S_{D7} = -\tau_7 \int d^8 \xi \left(e^{-\Phi} \sqrt{-\det(\mathcal{G}_{ab} + 2\pi\alpha' F_{ab})} - \frac{1}{8!} \epsilon^{i_1 \dots i_8} A_{i_1 \dots i_8} \right) \quad (39)$$

where $F_{ab} = \partial_a A_b - \partial_b A_a$, $\mathcal{G}_{ab} = \partial_{\xi^a} X^M \partial_{\xi^b} X^N G_{MN}$ ($a, b = 0 \sim 7$) and $\tau_7 = [(2\pi)^7 g_s \alpha'^4]^{-1}$ represent the induced metric and the tension of the D7-brane, respectively. The eight-form potential $A_{i_1 \dots i_8}$, which is the Hodge dual to the axion, couples to the D7-brane minimally. In terms of the Hodge dual field strength, $F_{(9)} = dA_{(8)}$ [20], the potential $A_{(8)}$ is obtained.

Taking the canonical gauge, we arrive at the following D7-brane action,

$$S_{D7} = -\tau_7 \int d^8 \xi \sqrt{\epsilon_3} \rho^3 \gamma(x)^3 a(t)^3 \left(A^4 e^{\Phi} \sqrt{1 + (w')^2} - \frac{\tilde{q}}{r^4} \right). \quad (40)$$

Then the equation of motion for $w(\rho)$ is obtained as

$$\begin{aligned} & \frac{w}{\rho + ww'} [\Phi' - \sqrt{1 + (w')^2} (\Phi + 4 \log A)'] \\ & + \frac{1}{\sqrt{1 + (w')^2}} \left[w' \left(\frac{3}{\rho} + (\Phi + 4 \log A)' \right) + \frac{w''}{1 + (w')^2} \right] = 0, \end{aligned} \quad (41)$$

where a prime denotes the derivative with respect to ρ . By solving this equation, we find the embedded configuration of the D7-brane. And from this solution, the quark mass, m_q , and the chiral condensate, $c = -\langle \bar{\Psi} \Psi \rangle$, are found through its asymptotic form at large ρ as

$$w(\rho) \sim m_q + \frac{c}{\rho^2}, \quad (42)$$

according to the gauge/gravity correspondence. However, we notice that the above asymptotic form, (42), must be modified. This is seen by expanding Eq. (41) in terms of the power series of $1/\rho^2$ by adding the power series of $\log(\rho)$ [12], and we obtain

$$w(\rho) \sim m_q + \frac{c_0 + 4m_q r_0^2 \log(\rho)}{\rho^2}. \quad (43)$$

This implies that the chiral condensate receives quantum corrections in the limit of $\rho \rightarrow 0$ as $c = c_0 + 4m_q r_0^2 \log(\rho)$. In other words, the conformal invariance of the 4d CFT is broken by the added chiral multiplet for the flavor quarks.

The solutions are obtained in terms of the above asymptotic form (43), and the results are shown in Fig. 2 for several values of m_q in the range $0 \leq m_q < 1$. We find $c > 0$ for all the solutions. This is understood from the repulsive force between D3- and D7-branes. The potential of the D7-brane near the D3-branes is given from the D7 action as

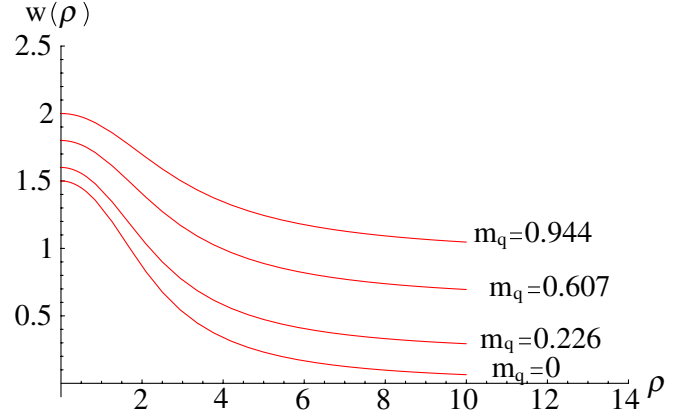


FIG. 2 (color online). Embedding solutions for $q = 1.0$ and $r_0 = 1.0$. The solutions are drawn for several values of m_q , where we have taken $R = 1$.

$$\begin{aligned} V(w) &= \tau_7 \left(A^4 e^{\Phi} - \frac{q}{r^4} - 1 \right) \\ &= \tau_7 \left\{ \left(1 + \frac{q}{3r_0^4} \right) \left(\frac{r_0}{r} \right)^8 + \dots \right\}. \end{aligned} \quad (44)$$

We find a strong repulsion near $r = 0$.

In Fig. 2, the solution of $m_q = 0$ with $c > 0$, which then breaks the chiral symmetry, is shown. On the other hand, the trivial solution with $w = 0$ and $m_q = 0$, which preserves the chiral symmetry since $c = 0$, also exists. The behaviors of the two solutions are very different near $\rho = 0$, although they are very similar at large ρ . We find for the trivial solution that the energy density of the D7-brane is divergent like $1/\rho^5$ at $\rho = 0$ since $V \sim 1/\rho^8$ near $\rho = 0$. On the other hand, for the solution of $m_q = 0$ with $c > 0$, the D7 energy density approaches zero like ρ^3 near $\rho = 0$, and as a result we obtain a finite energy after ρ integration in this case. Thus we can say that the chiral symmetry is spontaneously broken in the present case.

The second point to be addressed is that the solutions are far from the circle $r \sim r_0$. This is consistent with the stability of the fluctuations of the D7-brane since the U-shaped string configurations cannot be stretched up to $r = r_0$ as mentioned in the previous section.

V. POSSIBLE HADRON SPECTRUM

As shown in the previous section, the theory is in the quark confined phase and the U-shaped string configuration exists. In addition, the tension parameter of the string configuration depends on the cosmological constant λ and q . So the meson mass also depends on these parameters and m_q . However, the q dependence is rather small, and we expect that the mass spectra of the mesons are largely constrained by the geometry AdS₄.

We study these point by calculating the meson mass and comparing it with the one given by the field theory in AdS₄.

A. Meson spectrum

The meson spectrum is obtained by solving the equations of motion of the fields on the D7-brane. According to [12,23], first we consider the fluctuations of the scalar mesons, which are defined as

$$X^9 = \tilde{\phi}^9, \quad X^8 = w(\rho) + \tilde{\phi}^8,$$

and write the wave functions in the following factorized form,

$$\tilde{\phi}^k = \varphi^k(t, x^i) \phi_l^k(\rho) \mathcal{Y}_l(S^3) \quad (k = 9, 8),$$

where $\mathcal{Y}_l(S^3)$ denotes the spherical harmonic function on a three dimensional sphere with the angular momentum l . Then we study the linearized field equations for $\phi_l^9(\rho)$ and $\phi_l^8(\rho)$.

1. Solution for $w = 0$ and $q = 0$

At first, we consider the spectra of the mesons for a simple case where $w = 0$ and $q = 0$. In this case, the equations of motion for ϕ_l^8 and ϕ_l^9 have the following form,

$$\partial_\rho^2 \phi_l + \left(\frac{3}{\rho} - \frac{8r_0^2}{A\rho^3} \right) \partial_\rho \phi_l + \left[\frac{m^2 R^4}{A^2 \rho^4} - \frac{l(l+2)}{\rho^2} + \frac{8r_0^2}{A\rho^4} \right] \phi_l = 0, \quad (45)$$

where ϕ_l denotes ϕ_l^8 or ϕ_l^9 . The solution of this equation is obtained after some calculation as

$$\phi_l = (r_0^2 + \rho^2)^{-(3+\sqrt{9+\bar{m}^2})/2} \left\{ c_1 \rho^{4+l} F\left(\alpha, \alpha + l + 1, l + 2, -\frac{\rho^2}{r_0^2}\right) + c_2 \rho^{2-l} F\left(\alpha, \alpha - l - 1, -l, -\frac{\rho^2}{r_0^2}\right) \right\}, \quad (46)$$

$$\alpha = \frac{1}{2}(1 - \sqrt{9 + \bar{m}^2}), \quad \bar{m} = R^2 m / r_0, \quad (47)$$

where c_1 and c_2 are arbitrary constants and F denotes the hypergeometric function. In order to have a convergent solution ϕ at small ρ , we must take $c_2 = 0$. And from the condition at large ρ , α must be set as

$$\alpha + l + 1 = -n, \quad n = 0, 1, 2, \dots \quad (48)$$

The solution is expressed by the finite power series of ρ due to this condition, and we find the normalizability of the wave function. Then we find the following result,

$$m^2 = -\lambda(l+n)(l+n+3). \quad (49)$$

This represents precisely the same spectrum as the one obtained by Avis, Isham, and Storey [14] in AdS₄ for scalar fields. This point is important since the mass scale λ in Eq. (49) is largely modified for the case of $w \neq 0$ and

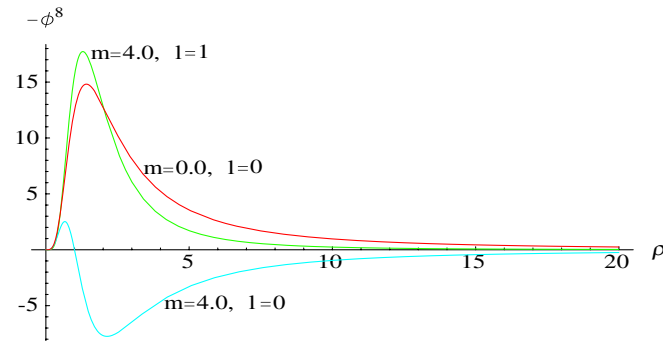


FIG. 3 (color online). The solutions for $w = q = 0$. The ones for (i) $m = 0, l = 0$, (ii) $m^2 = -4\lambda, l = 0$, and (iii) $m^2 = -4\lambda, l = 1$ are shown for $r_0 = 1.0$ and $R = 1$, then $-\lambda = 4$. The scale of the wave function for (iii) is expressed by multiplying by the extra factor 10^{-4} compared to the other two functions.

$q \neq 0$ as shown in the next subsection. In the present case, $w = 0$ and $q = 0$; then the quantum effects coming from the gauge interactions are all suppressed. Hence the above formula is obtained.

We show the typical wave functions for $m^2 = 0$ and $m^2 = -4\lambda$ in Fig. 3. The mass eigenvalue $m = 4$ is obtained by the two degenerate states, $(n, l) = (0, 1)$ and $(1, 0)$, whose wave functions are shown in Fig. 3. They have different functional forms. In the next subsection, we can see the splitting of these degenerate masses by introducing nonzero $w(\rho)$ and q . Therefore, they deviate from the above mass formula (49).

These solutions preserve the chiral symmetry since the chiral condensate vanishes in the case of $w = 0$. However, they are not realized from the energy principle since the one of $w \neq 0$ with the same boundary condition at $\rho = \infty$ is preferred; then the chiral symmetry is spontaneously broken. The mass spectra in this realistic case $w \neq 0$ are examined by the numerical analyses in the next subsection, and we can see the details of the deviations of the meson spectra.

2. Solution for $w \neq 0$

Next, we get the linearized field equations for $\phi_l^9(\rho)$ and $\phi_l^8(\rho)$ for $w \neq 0$ as follows:

$$\begin{aligned} \partial_\rho^2 \phi_l^9 + \frac{1}{L_0} \partial_\rho(L_0) \partial_\rho \phi_l^9 \\ + (1 + w^{l^2}) \left[\left(\frac{R}{r} \right)^4 \frac{m_0^2}{A^2} - \frac{l(l+2)}{\rho^2} - 2K_{(1)} \right] \phi_l^9 \\ + (1 + w^{l^2})^{1/2} \frac{1}{r} \frac{\partial \Phi}{\partial r} \phi_l^9 = 0, \quad (50) \end{aligned}$$

$$L_0 = \rho^3 e^{\Phi} A^4 \frac{1}{\sqrt{1+w^2}}, \quad K_{(1)} = \frac{1}{e^{\Phi} A^4} \partial_{r^2}(e^{\Phi} A^4) \quad (51)$$

and

$$\begin{aligned} \partial_\rho^2 \phi_l^8 + \frac{1}{L_1} \partial_\rho(L_1) \partial_\rho \phi_l^8 + (1+w^2) \left[\left(\frac{R}{r} \right)^4 \frac{m_8^2}{A^2} - \frac{l(l+2)}{\rho^2} - 2(1+w^2)(K_{(1)} + 2w^2 K_{(2)}) \right] \phi_l^8 \\ + (1+w^2)^{3/2} \left[\left(2rK_{(1)} \frac{\partial \Phi}{\partial r} + \frac{\partial^2 \Phi}{\partial r^2} \right) \frac{w^2}{r^2} + \frac{\partial \Phi}{\partial r} \frac{\rho^2}{r^3} \right] \phi_l^8 = -2 \frac{1}{L_1} \partial_\rho(L_0 w w' K_{(1)}) \phi_l^8, \end{aligned} \quad (52)$$

$$L_1 = \frac{L_0}{1+w^2}, \quad K_{(2)} = \frac{1}{e^{\Phi} A^4} \partial_{r^2}^2(e^{\Phi} A^4), \quad (53)$$

where the four dimensional masses m_9 and m_8 are defined by

$$-\square_4 \varphi^k = \ddot{\varphi}^k + 3 \frac{\dot{a}}{a} \dot{\varphi}^k - \frac{1}{a^2 \gamma^3} \partial_i(\gamma \partial_i \varphi^k) = -m_k^2 \varphi^k \quad (k=9,8). \quad (54)$$

In deriving the above equations (50) of ϕ_l^9 and (52) of ϕ_l^8 , we used

$$r^2 = \rho^2 + (\phi_l^8)^2 + (\phi_l^9)^2 + w^2 + 2w\phi_l^9. \quad (55)$$

But we should notice here that the variable r in the above field equations is understood as $r^2 = \rho^2 + w^2$ since we are considering the linearized equations.

In Figs. 4(a) and 4(b), the numerical results of the mass eigenvalues, m_9 and m_8 , are plotted as functions of m_q . These values are all for the nodeless solutions, i.e. for the lowest mass states. It seems that they approach the same values at large m_q [23]. On the other hand, as seen from Figs. 5(a) and 5(b), we have verified that the relation

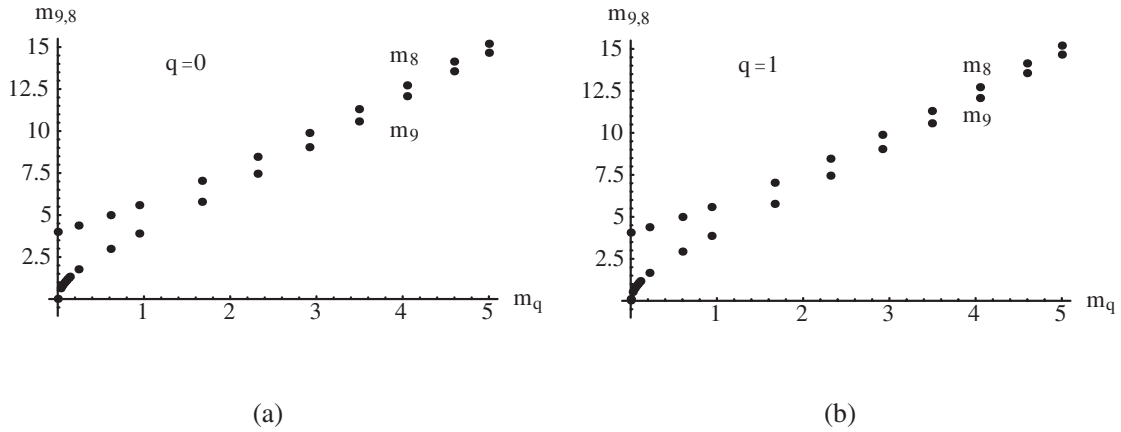


FIG. 4. The values of $m_{9,8}$ are shown at various m_q for $l=n=0$, $r_0=1.0$ and $R=1$, and (a) $q=0$, (b) $q=1$.

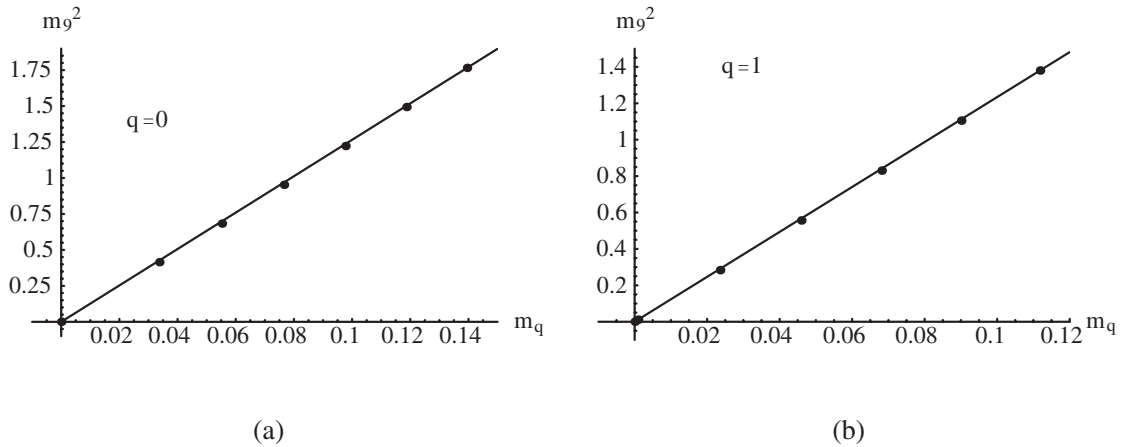


FIG. 5. The values of m_9^2 are shown at various m_q for $l=n=0$, $r_0=1.0$ and $R=1$, and (a) $q=0$, (b) $q=1$.

$m_9^2 \propto m_q$ holds very accurately in the small m_q region for both $q = 0$ and $q = 1$. This fact assures that $\phi_{l=0}^9$ is the Nambu-Goldstone boson as expected, and implies a kind of GellMann-Oakes-Renar-like relation.

Next, let us compare our numerical results with the mass formula of scalars given in AdS₄ by Avis, Isham, and Storey [14]. In Ref. [14], the masses of scalars in AdS₄ are given by

$$m_l^2 = K(I-3)I, \quad I > 2, \quad (56)$$

where m_l is written for the case without the conformal coupling of the scalar and gravity, and I is given by (i) $2 < I < 5/2$ or (ii) $I = 3, 4, 5, \dots$. Case (i) represents a continuous spectrum, while case (ii) represents a discrete one. The parameter K is related to our λ as

$$K = {}^{(4)}R/12 = -\lambda, \quad (57)$$

where ${}^{(4)}R$ denotes the four dimensional scalar curvature.

Let us begin with eigenvalues at $m_q = 10^{-5}$ shown in Fig. 6. Since obtained eigenvalues have zero or finite nodes (denoted by n) or integer l , they correspond to case (ii) of the mass formula (56). The continuous spectrum (i), which corresponds to tachyons, does not exist in our case. It seems somewhat curious from the viewpoint of AdS/CFT correspondence that the corresponding spectrum to (i) does not exist. And we consider that the ground state for m_9^2 corresponds to $I = 3$ since it is massless, while the ground state for m_8^2 corresponds to $I = 4$ since it is massive. Obtained values are in very good agreement with formula (56) for the ground states. Their values are $m_9^2 = 1.31 \times 10^{-4}$ for $q = 0$ and 1.12×10^{-4} for $q = 1$, while $m_8^2 = 16.0$ for $q = 0$ and 16.5 for $q = 1$.

However, the numerical results deviate from the mass formula for the excited states with respect to n and l . We can see that the deviation from formula (56) becomes large

with increasing $n(l)$. These deviations might be reduced to the gauge interactions between the quark and antiquark which make a bound state. As shown in the previous subsection, formula (56) is reproduced when we set $w = 0$. On the other hand, the mass deviates from this formula when we take into account nontrivial w . Since the profile function w includes the quark mass and the vacuum expectation value of $\bar{\Psi}\Psi$ and other information of the interaction between the quarks and the gauge fields, then the deviation observed is naturally understood as the reflection from the gauge interactions to the meson mass. We can see this effect through the change of the mass scale in the mass formula as shown below.

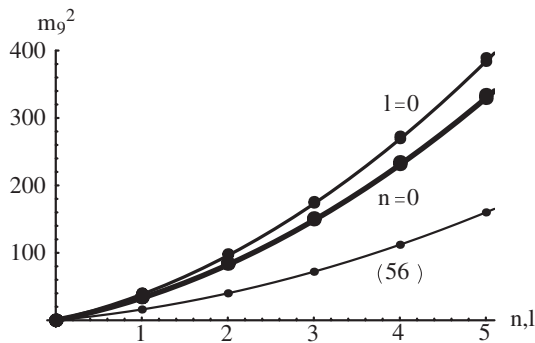
Fortunately, obtained values are almost degenerate for $q = 0$ and $q = 1$ as seen from Fig. 6. So, we attempt to fit the data at the present stage by changing K by hand such that the obtained values for the highest excited states with $q = 0$ are reproduced. The reason why we fit in such a way is as follows: since obtained values for ground states are in good agreement with the mass formula (56) and deviate for higher excited states, we want to know, conversely, deviations for lower lying states when the above-mentioned fittings are performed. The results are as follows for n excitations with $l = 0$,

$$K_n^{(0)} = 2.40K \quad \text{for } m_9^2, \quad K_n^{(0)} = 1.85K \quad \text{for } m_8^2,$$

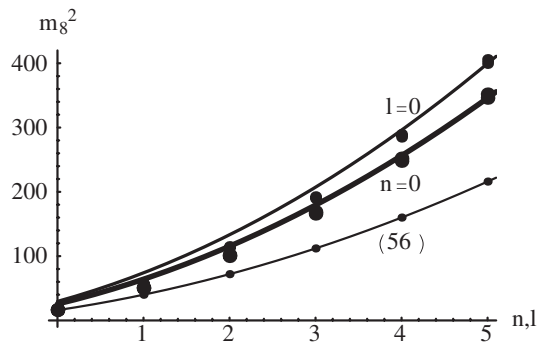
and for l excitations with $n = 0$,

$$K_l^{(0)} = 2.06K \quad \text{for } m_9^2, \quad K_l^{(0)} = 1.60K \quad \text{for } m_8^2.$$

The coincidence is very (rather) good for m_9^2 (m_8^2) so that we may conclude that I dependence of formula (56) is trustable. But it should be noted that n excitations and l excitations are split because $K_n^{(0)}$ and $K_l^{(0)}$ take different values. Although the mass formula (49) is degenerate for



(a) m_9^2 vs n, l at $m_q = 10^{-5}$ with $r_0 = 1.0$, $R = 1$ and $\lambda = -4$



(b) m_8^2 vs n, l at $m_q = 10^{-5}$ with $r_0 = 1.0$, $R = 1$ and $\lambda = -4$

FIG. 6. Small points and the thin curve correspond to formula (56). Second-largest points and second-thickest curves represent the obtained values and a fitted curve, respectively, for node (n) excitations with $l = 0$, while large points and thick curves represent obtained values and a fitted curve, respectively, for l excitations with $n = 0$.

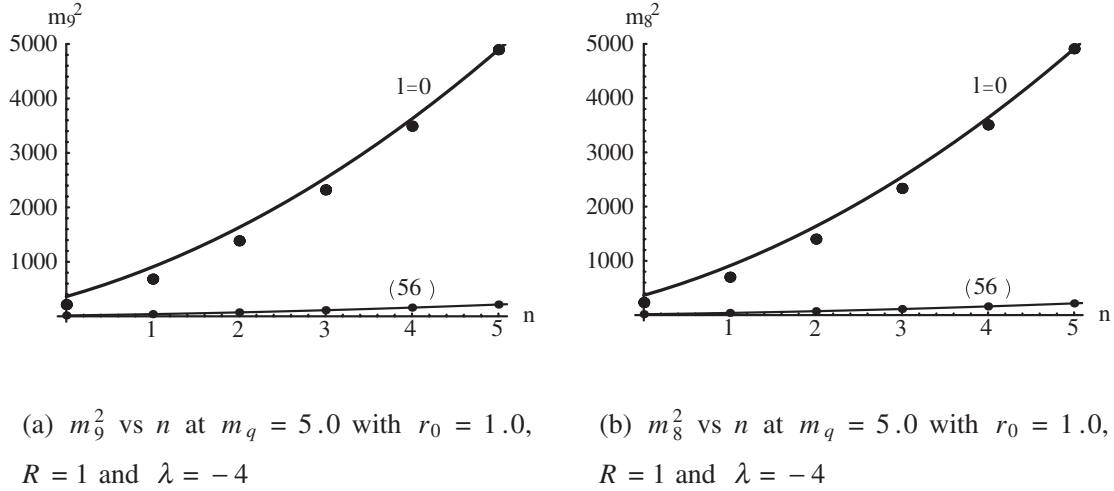


FIG. 7. Points and the curve represent the obtained values and a fitted curve, respectively, for node (n) excitations with $l = 0$. The lower lying points and the thin curve correspond to the mass formula (56).

n excitations and l excitations, it is obtained for $w = 0$, which is not the real solution. The real solution is $w \neq 0$ for $m_q = 0$ and formula (49) does not contradict with the splitting mentioned above.

Next we study the case of large m_q . In the case of $m_q = 5.0$, obtained values are rather large compared with the ones given by the mass formula (56) as shown in Fig. 7. This is because $K = -\lambda$ is independent of m_q . It should be changed as $K_{(n,l)} \rightarrow \tilde{K}_{(n,l)}(\lambda, m_q, g_{YM}^2, \dots)$. But the definite and detailed form of \tilde{K} is unknown at the present stage so that we again choose the fitting by changing K as $m_q = 10^{-5}$ case. The results are as follows for n excitations with $l = 0$,

$$K_n^{(5)} = 22.7K \quad \text{for } m_9^2, \quad K_n^{(5)} = 22.7K \quad \text{for } m_8^2.$$

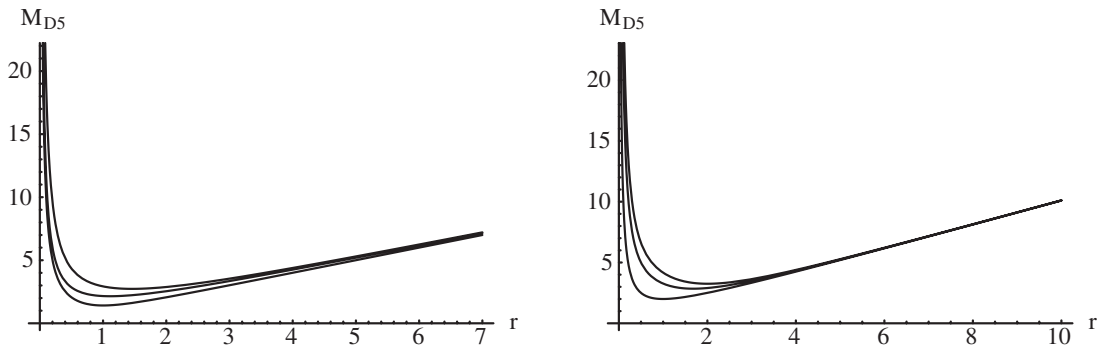
The coincidences are relatively good so that we may again conclude that l dependence of formula (56) is trustable. To derive a more realistic mass formula is a future problem.

B. Baryon

It has been shown that baryons correspond to D5-branes wrapped around the compact manifold M_5 [24,25]. Here we assume it to be S^5 . The brane action of such a D5 probe is

$$S_{D5} = -\tau_5 \int d^6 \xi e^{-\Phi} \sqrt{\mathcal{G}}, \quad (58)$$

where $(\xi_i) = (X^0, X^5 \sim X^9)$, τ_5 represents the tension of the D5-brane, and $\mathcal{G} = -\det(\mathcal{G}_{i,j})$ for the induced metric $\mathcal{G}_{ij} = \partial_{\xi^i} X^M \partial_{\xi^j} X^N G_{MN}$. The mass of the wrapped D5-brane is then



(a) The curves show $M_{D5}|_{\lambda=0}$, $M_{D5}|_{\lambda=-4}$, and $M_{D5}|_{\lambda=-5.76}$, respectively, from bottom to top $\tilde{q} = 1$.
(b) For $\lambda = -4$, $M_{D5}|_{\tilde{q}=0}$, $M_{D5}|_{\tilde{q}=10}$, and $M_{D5}|_{\tilde{q}=20}$, are shown from bottom to top.

FIG. 8. The D5-brane mass $M_{D5}(r)$ as a function of r for $R = 1$ and $\tau_5 = 1/\pi^3 R^4$.

$$M_{D5}(r, \lambda) = \tau_5 e^{-\Phi} \sqrt{G} = \tau_5 \pi^3 R^4 r A(r) e^{\Phi/2}. \quad (59)$$

Before seeing the λ dependence of this quantity, we consider the case of $\lambda = 0$,

$$M_{D5}(r, 0) = \tau_5 \pi^3 R^4 r \sqrt{1 + \frac{\tilde{q}}{r^4}}, \quad (60)$$

where \tilde{q} is given by (12). This has a global minimum at $r = r_{\min} = \tilde{q}^{1/4}$. Its value is given as $M_{D5}(r_{\min}) = \tau_5 \pi^3 R^4 (4\tilde{q})^{1/4}$, and this is regarded as the baryon mass here. In the 4d Minkowski limit, namely, at $\lambda = 0$, the baryon mass is induced by \tilde{q} , i.e. by the gauge-field condensate.

In the presence of λ , namely, in AdS₄, the minimum of M_{D5} appears even if $q = 0$. For $q = 0$, we obtain $M_{D5}(r = r_0, 0)/(\tau_5 \pi^3 R^4) = 2r_0$ as the minimum, which is realized at $r = r_0$.

Figures 8(a) and 8(b) show the r dependence of $M_{D5}(r)$ for three values of λ and q , respectively. For any finite values of λ , even if $q = 0$, there exists a minimum at an appropriate point of r , and the minimum value of M_{D5} increases with λ and q . This point is consistent with the above analysis of mesons, whose mass increases with these parameters.

VI. SUMMARY

In this paper, the nonperturbative properties of the gauge theories in AdS₄ are studied in dual supergravity by including light flavor quarks, which are introduced by a D7-brane embedding.

In our model, in the Minkowski space limit ($r_0 \rightarrow 0$), we have $g_{\text{YM}}^2 = 1 + \frac{\tilde{q}}{r^4}$, which is equivalent to the supersymmetric solution given previously [10]. In this limit, the quark is confined due to the strong YM coupling constant in the infrared limit, $r \rightarrow 0$, for $\tilde{q} > 0$. On the other hand, in the AdS₄ space-time (finite r_0), we find $g_{\text{YM}}^2 \rightarrow 1 + \frac{q}{3}$ in the infrared limit, $r \rightarrow 0$. While this coupling constant seems small to get the quark confinement, we find the confinement by calculating the Wilson loop which leads to the area law and the divergent effective single quark mass. These results are obtained even if $q = 0$, and the important factor to get the confinement is reduced to the warp factor $A(r)$ which diverges at $r = 0$ for finite r_0 . In this sense, contrary to the case of Minkowski space-time, the gauge

interaction does not play any important role for the quark confinement in the AdS₄ case. The important point is the geometry itself.

As for the chiral symmetry, we could expect its spontaneous breaking due to the repulsion between the D7- and the D3-branes. Actually, we could find a numerical solution for the profile function $w(\rho)$, with $m_q = 0$ and $c > 0$, and it has a finite D7 energy which is obtained after ρ integration. On the other hand, the trivial solution $w(\rho) = 0$, the one of $m_q = c = 0$, leads to an infinite D7 energy due to the infinite repulsion at $r = 0$ due to the D3-branes. We thus find the spontaneous breaking of the chiral symmetry.

In the present case, for all the solutions of $w(\rho)$, we need a correction like $m_q \lambda \log(\rho)$ to the expectation value of $\langle \bar{\Psi} \Psi \rangle$. This is expected when conformal symmetry and supersymmetry are broken even in the UV limit as in the present model. Since this correction is proportional to m_q , the loop corrections of the massive hypermultiplet added to CFT would be responsible for this result.

The scalar meson spectra are calculated and we could find the Goldstone boson due to the chiral symmetry breaking. The coincidence of the obtained masses to the mass formula given in Ref. [14] is very good for the lowest states. On the other hand, for the excited states, our results deviate from the mass formula. However, when we modify K by hand in the mass formula (56), we find better coincidences. This is interpreted as the reflection of the gauge interaction between the quark and antiquark when they form bound states.

The baryon mass is studied by regarding it as the energy of the D5-brane, wrapped on S^5 , embedded at a stable point with respect to the coordinate r . For any finite values of λ , even if $q = 0$, we find a minimum or a stable point at an appropriate point of r . This is consistent with the meson case.

ACKNOWLEDGMENTS

The authors would like to thank Carlos Nunez for useful comments. K.G. is grateful to him for interesting discussions. This work has been supported in part by the Grants-in-Aid for Scientific Research (No. 13135223) of the Ministry of Education, Science, Sports, and Culture of Japan.

[1] J. M. Maldacena, Adv. Theor. Math. Phys. **2**, 231 (1998); Int. J. Theor. Phys. **38**, 1113 (1999); S. S. Gubser, I. R. Klebanov, and A. M. Polyakov, Phys. Lett. B **428**, 105

(1998); E. Witten, Adv. Theor. Math. Phys. **2**, 253 (1998); A. M. Polyakov, Int. J. Mod. Phys. A **14**, 645 (1999).

[2] A. Karch and E. Katz, J. High Energy Phys. 06 (2002) 043.

- [3] M. Kruczenski, D. Mateos, R. C. Myers, and D. J. Winters, *J. High Energy Phys.* 07 (2003) 049.
- [4] M. Kruczenski, D. Mateos, R. C. Myers, and D. J. Winters, *J. High Energy Phys.* 05 (2004) 041.
- [5] J. Babington, J. Erdmenger, N. J. Evans, Z. Guralnik, and I. Kirsch, *Phys. Rev. D* **69**, 066007 (2004).
- [6] N. J. Evans and J. P. Shock, *Phys. Rev. D* **70**, 046002 (2004).
- [7] T. Sakai and J. Sonnenschein, *J. High Energy Phys.* 09 (2003) 047.
- [8] C. Nunez, A. Paredes, and A. V. Ramallo, *J. High Energy Phys.* 12 (2003) 024.
- [9] T. Sakai and S. Sugimoto, *Prog. Theor. Phys.* **113**, 843 (2005); **114**, 1083 (2005).
- [10] K. Ghoroku and M. Yahiro, *Phys. Lett. B* **604**, 235 (2004).
- [11] K. Ghoroku, T. Sakaguchi, N. Uekusa, and M. Yahiro, *Phys. Rev. D* **71**, 106002 (2005).
- [12] K. Ghoroku, M. Ishihara, and A. Nakamura, *Phys. Rev. D* **74**, 124020 (2006).
- [13] T. Hirayama, *J. High Energy Phys.* 06 (2006) 013.
- [14] S. J. Avis, C. J. Isham, and D. Storey, *Phys. Rev. D* **18**, 3565 (1978).
- [15] A. Karch and L. Randall, *J. High Energy Phys.* 05 (2001) 008.
- [16] M. Porrati, *J. High Energy Phys.* 04 (2002) 058.
- [17] B. A. Burrington and J. T. Liu, *J. High Energy Phys.* 03 (2004) 059.
- [18] A. Kehagias and K. Sfetsos, *Phys. Lett. B* **456**, 22 (1999).
- [19] H. Liu and A. A. Tseytlin, *Nucl. Phys.* **B553**, 231 (1999).
- [20] G. W. Gibbons, M. B. Green, and M. J. Perry, *Phys. Lett. B* **370**, 37 (1996).
- [21] H. Lu, C. N. Pope, and J. Rahmfeld, *J. Math. Phys. (N.Y.)* **40**, 4518 (1999).
- [22] S. Gubser, hep-th/9902155.
- [23] I. Brevik, K. Ghoroku, and A. Nakamura, *Int. J. Mod. Phys. D* **15**, 57 (2006).
- [24] D. J. Gross and H. Ooguri, *Phys. Rev. D* **58**, 106002 (1998).
- [25] E. Witten, *J. High Energy Phys.* 07 (1998) 006.